ISSN 1674-1056
http://cpb.iphy.ac.cn
http://iopscience.iop.org/cpb
中国物理 B
Chinese Physics
中国物理
Chinese Physics B

The effect of surface oxygen vacancy defects on the performance of ZnO quantum dots ultraviolet photodetector

Hongyu Ma(马宏宇), Kewei Liu(刘可为), Zhen Cheng(程祯), Zhiyao Zheng(郑智遥), Yinzhe Liu(刘寅哲), Peixuan Zhang(张培宣), Xing Chen(陈星), Deming Liu(刘德明), Lei Liu(刘雷), and Dezhen Shen(申德振)
Citation:CChin. Phys. B, 2021, 30 (**8**): 087303. DOI: 10.1088/1674-1056/ac0131
Journal homepage: http://cpb.iphy.ac.cn; http://iopscience.iop.org/cpb

What follows is a list of articles you may be interested in

Modeling, simulations, and optimizations of gallium oxide on gallium-nitride Schottky barrier diodes

Tao Fang(房涛), Ling-Qi Li(李灵琪), Guang-Rui Xia(夏光睿), and Hong-Yu Yu(于洪宇)
Chin. Phys. B, 2021, 30 (**2**): 027301. DOI: 10.1088/1674-1056/abc0dd

Dispersion of exciton-polariton based on ZnO/MgZnO quantum wells at room temperature

Huying Zheng(郑湖颖), Zhiyang Chen(陈智阳), Hai Zhu(朱海), Ziying Tang(汤梓荧), Yaqi Wang(王亚琪), Haiyuan Wei(韦海园), Chongxin Shan(单崇新)
Chin. Phys. B, 2020, 29 (**9**): 097302. DOI: 10.1088/1674-1056/ab99b3

Influence of $Zr_{50}Cu_{50}$ thin film metallic glass as buffer layer on the structural and optoelectrical properties of AZO films

Bao-Qing Zhang(张宝庆), Gao-Peng Liu(刘高鹏), Hai-Tao Zong(宗海涛), Li-Ge Fu(付丽歌), Zhi-Fei Wei(魏志飞), Xiao-Wei Yang(杨晓炜), Guo-Hua Cao(曹国华)
Chin. Phys. B, 2020, 29 (**3**): 037303. DOI: 10.1088/1674-1056/ab6c50

Effects of active layer thickness on performance and stability of dual-active-layer amorphous InGaZnO thin-film transistors

Wenxing Huo(霍文星), Zengxia Mei(梅增霞), Yicheng Lu(卢毅成), Zuyin Han(韩祖银), Rui Zhu(朱锐), Tao Wang(王涛), Yanxin Sui(隋妍心), Huili Liang(梁会力), Xiaolong Du(杜小龙)
Chin. Phys. B, 2019, 28 (**8**): 087302. DOI: 10.1088/1674-1056/28/8/087302

Energy band alignment at Cu_2O/ZnO heterojunctions characterized by *in situ* x-ray photoelectron spectroscopy

Yan Zhao(赵妍), Hong-Bu Yin(尹泓卜), Ya-Jun Fu(符亚军), Xue-Min Wang(王雪敏), Wei-Dong Wu(吴卫东)
Chin. Phys. B, 2019, 28 (**8**): 087301. DOI: 10.1088/1674-1056/28/8/087301

Effect of surface oxygen vacancy defects on the performance of ZnO quantum dots ultraviolet photodetector*

Hongyu Ma(马宏宇)[1,2], Kewei Liu(刘可为)[1,2,†], Zhen Cheng(程祯)[1], Zhiyao Zheng(郑智遥)[1,2], Yinzhe Liu(刘寅哲)[1,2], Peixuan Zhang(张培宣)[1,2], Xing Chen(陈星)[1], Deming Liu(刘德明)[1], Lei Liu(刘雷)[1,2], and Dezhen Shen(申德振)[1,2,‡]

[1] *State Key Laboratory of Luminescence and Applications, Changchun Institute of Optics, Fine Mechanics and Physics, Chinese Academy of Sciences (CAS), Changchun* 130033, *China*

[2] *Center of Materials Science and Optoelectronics Engineering, University of Chinese Academy of Sciences, Beijing* 100049, *China*

(Received 6 May 2021; revised manuscript received 11 May 2021; accepted manuscript online 14 May 2021)

The slower response speed is the main problem in the application of ZnO quantum dots (QDs) photodetector, which has been commonly attributed to the presence of excess oxygen vacancy defects and oxygen adsorption/desorption processes. However, the detailed mechanism is still not very clear. Herein, the properties of ZnO QDs and their photodetectors with different amounts of oxygen vacancy (V_O) defects controlled by hydrogen peroxide (H_2O_2) solution treatment have been investigated. After H_2O_2 solution treatment, V_O concentration of ZnO QDs decreased. The H_2O_2 solution-treated device has a higher photocurrent and a lower dark current. Meanwhile, with the increase in V_O concentration of ZnO QDs, the response speed of the device has been improved due to the increase of oxygen adsorption/desorption rate. More interestingly, the response speed of the device became less sensitive to temperature and oxygen concentration with the increase of V_O defects. The findings in this work clarify that the surface V_O defects of ZnO QDs could enhance the photoresponse speed, which is helpful for sensor designing.

Keywords: ZnO, quantum dots, ultraviolet photodetector, oxygen vacancy

PACS: 73.61.Ga, 85.60.Gz, 85.35.Be **DOI:** 10.1088/1674-1056/ac0131

1. Introduction

Ultraviolet (UV) detection technology has been broadly applicated in military and civilian fields.[1–5] ZnO, a direct wide bandgap semiconductor, has been commonly regarded as one of the most promising materials for the fabrication of UV photodetectors due to its intrinsic visible blindness, strong radiation hardness, and high chemical and thermal stability.[6–9] Till now, ZnO-based UV photodetectors using the bulk, thin film or nanostructures have been demonstrated and investigated with high responsivity, long-term stability, and excellent wavelength selectivity. In general, the dimensionality and the shape of the materials play essential roles in their properties and applications. ZnO quantum dots (QDs), as a zero-dimensional nanostructure, have been received considerable interest due to their high specific surface area, size-tunable bandgap, and quantum-sized effect, which could improve the photodetection and photoresponse performance.[10–22] Although ZnO QDs photodetectors have made significant progress, their response time and recovery time are far from ideal.[23–31] It is generally accepted that the slow response and recovery speeds are dominated by the persistent photoconductivity (PPC) effect and oxygen adsorption/desorption processes.[32–34] However, it is difficult to explain that under vacuum or oxygen-free conditions, the response and recovery speed of ZnO UV photodetectors are actually much slower than that in an oxygen-rich atmosphere.[24,35–37]

Oxygen vacancy (V_O) defects are mainly considered as shallow donor level defects, and they could also act as molecular oxygen adsorption sites on the surface.[38–40] Therefore, studying ZnO QDs photodetectors with different concentrations of oxygen vacancy defects will help clarify the core mechanism of its slow response speed. Previous reports have indicated that H_2O_2 treatment can remove the surface V_O.[41] Herein, ZnO QDs UV photodetectors with and without H_2O_2 solution treatment have been demonstrated and investigated. The x-ray photoelectron spectroscopy (XPS) analysis, photoluminescence (PL), and PL excitation (PLE) spectra suggested that V_O concentration of ZnO QDs decreased after H_2O_2 solution treatment. The H_2O_2 solution-treated device exhibits a higher photocurrent and a lower dark current. More interestingly, the response speed of the devices with and without H_2O_2 solution treatment shows different dependences on surrounding atmosphere and on temperature, and the pristine device with more surface V_O defects has a quicker response speed. The detailed mechanism of how the oxygen vacancy defects

*Project supported by the National Natural Science Foundation of China (Grant Nos. 62074148, 61875194, 11727902, 12074372, 11774341, 11974344, 61975204, and 11804335), the Youth Innovation Promotion Association of the Chinese Academy of Sciences (Grant No. 2020225), the Open Project of the State Key Laboratory of Luminescence and Applications (Grant Nos. SKLA-2020-02 and SKLA-2020-06).

†Corresponding author. E-mail: liukw@ciomp.ac.cn

‡Corresponding author. E-mail: shendz@ciomp.ac.cn

© 2021 Chinese Physical Society and IOP Publishing Ltd

affect the detection performance of the device has been discussed. Our findings in this paper point out the direction for the realization of high-performance nanostructured ultraviolet detectors.

2. Experimental details

2.1. Preparation of ZnO QDs

ZnO QDs were prepared through solution-processed by using $Zn(CH_3COO)_2{\cdot}2H_2O$ and KOH as the raw material. 1.1-g (5 mmol) $Zn(CH_3COO)_2{\cdot}2H_2O$ was dissolved in 30-mL absolute ethanol and the solution was then continuously stirred at 70 °C for 1 hour. Afterwards, the solution was cooled down to 0 °C through the ice water bath. Meanwhile, 0.41-g (7 mmol) KOH was also dissolved in 3-mL absolute ethanol, which was slowly added into the solution of $Zn(CH_3COO)_2{\cdot}2H_2O$. After the mixed solution changed from turbid to clear in only few seconds, a large amount of n-Hexane was immediately added into the mixed solution until the ZnO QDs were obtained as white precipitate. The precipitate was collected and washed with ethanol for three times. Finally, ZnO QDs were re-dispersed into absolute ethanol with a concentration of 1 mol/L.

2.2. Fabrication of ZnO QDs photodetectors

The *c*-face sapphire substrate was cleaned by ultrasonic cleaning with trichloroethylene, acetone, and ethanol sequentially, and then the Au interdigital electrodes with 10 μm in width, 500 μm in length, and 10 μm in space were deposited on it by the photolithography and lift-off techniques. After that, ZnO QDs solution was spin-coated on the electrodes with a rotation rate of 2000 rpm for 20 s. The samples were dried on a hotplate at 90 °C for 10 min to form the ZnO QDs metal–semiconductor–metal (MSM) photodetectors. In addition, to fabricate the H_2O_2 solution-treated devices, the pristine ZnO QDs UV detector was immersed in H_2O_2 solution at room temperature for 5 seconds followed by a secondary drying process.

2.3. Characterizations of the materials and devices

The morphology of the ZnO QDs and their films were characterized by transmission electron microscopy (TEM) (FEI Talos F200s) and scanning electron microscope (SEM) (Hitachi S-4800). The PL and PLE spectra were analyzed by a fluorescence spectrophotometer (Hitachi F-7000) with a 150-W Xe lamp and a monochromator as the excitation source. The XPS measurements were carried out by a commercial XPS spectrometer (Thermo ESCALAB 250). Current–voltage (*I*–*V*) and time-dependent photocurrent (*I*–*t*) measurements of the photodetectors were performed by a semiconductor parameter analyzer (Keithely 2200). The response spectra were measured using a 200-W UV-enhanced Xe lamp and a monochromator.

3. Results and discussion

The TEM images of ZnO QDs with and without H_2O_2 solution treatment are shown in Figs. 1(a) and 1(b). The morphology of pristine ZnO QDs is uniformly spherical and the diameter of ZnO QDs is about 4 nm. Moreover, it can be seen that the size of the ZnO QDs was almost unchanged after the H_2O_2 treatment. Figures 1(c) and 1(d) present the SEM images of pristine ZnO QDs film and the same film treated by H_2O_2. It is obvious that the surface of the sample after H_2O_2 treatment becomes slightly rougher. Meanwhile, the H_2O_2 solution treatment could hardly change the thickness of ZnO QDs film (see the insets of Figs. 1(c) and 1(d)). The TEM and SEM results suggest that the 5-second H_2O_2 solution treatment used in this work did not cause obvious corrosion of the ZnO QDs and its film.

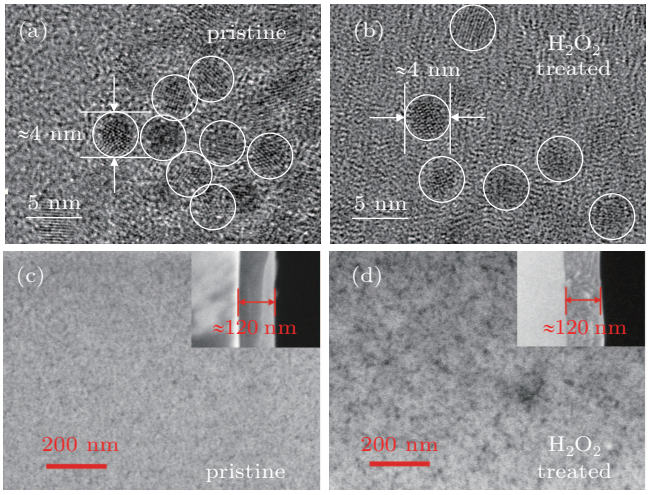


Fig. 1. TEM images of pristine (a) and H_2O_2-treated (d) ZnO QDs. Top-view and side-view (inset) SEM images of pristine (c) and H_2O_2-treated (d) ZnO QDs films.

The XPS spectra in the binding energy (BE) range from 0 eV to 1200 eV of the pristine and H_2O_2-treated ZnO QDs films are shown in Fig. 2(a). The XPS spectra have been calibrated by taking the C1s peak of carbon (284.6 eV) as Ref. [42]. The peak positions of both the pristine and H_2O_2-treated ZnO QDs films are similar, and all the peaks labelled in the XPS spectra can be ascribed to Zn and O in ZnO, and the C is from carbon contamination. There are no other impurities introduced. As the crucial point of our research, figures 2(b) and 2(c) show the XPS O1s peak of the pristine ZnO QDs film and the H_2O_2 solution-treated film, respectively. Both curves exhibit obvious asymmetry and then deconvolution was performed by the Gauss fitting. Clearly, both O1s peaks can be decomposed into two components centered at $\sim$ 530 eV (O_I) and $\sim$ 531 eV (O_{II}). The peak at $\sim$ 530 eV is associated with the lattice oxygen in wurzite-type ZnO, and the peak at

$\sim$ 531 eV can be attributed to the oxygen deficient regions on the surface of ZnO.[43] It should be noted that oxygen peaks at $\sim$ 530 eV and $\sim$ 531 eV of pristine ZnO QDs film accounted for 33.74% and 66.26% of the total O1s area, respectively. After the H_2O_2 solution treatment, the peaks at $\sim$ 530 eV and $\sim$ 531 eV accounted for 66.34% and 33.66% of the total O1s area, respectively, illustrating the V_O defects in the ZnO QDs film were effectively filled by the H_2O_2 treatment.

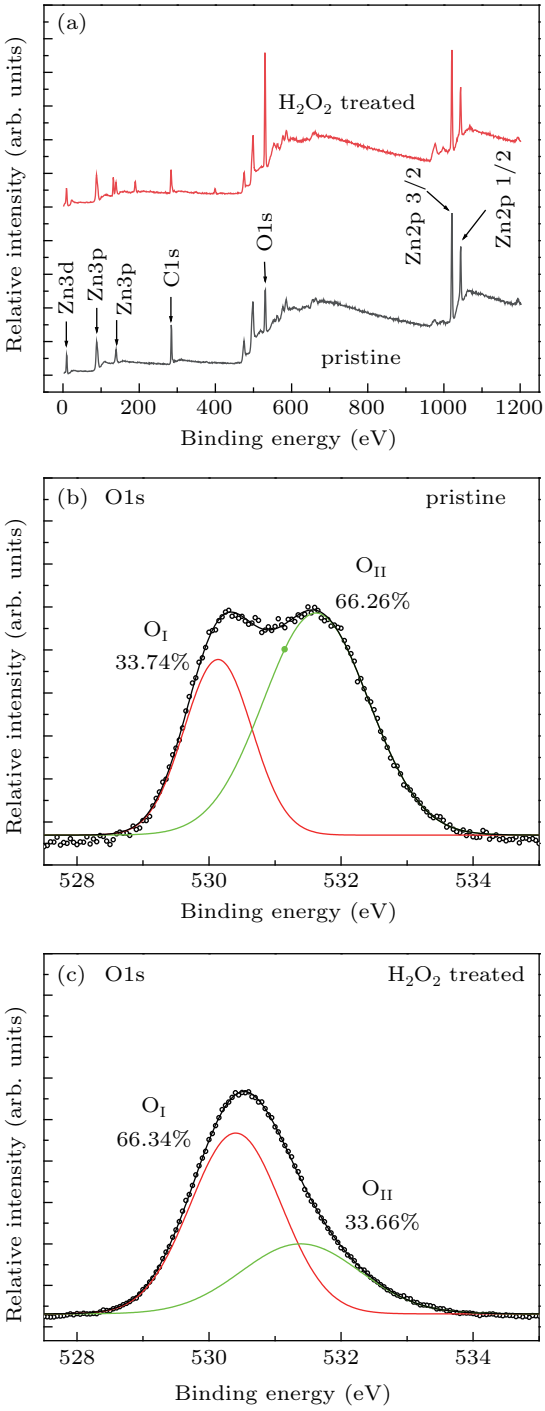


Fig. 2. (a) The evolution of XPS survey spectra of pristine (black) and H_2O_2-treated (red) ZnO QDs films in a full 1200-eV binding energy range. The evolution of XPS O1s core level lines of pristine (b) and H_2O_2-treated (c) ZnO QDs films.

Figure 3(a) shows the PL spectra at room temperature of the pristine ZnO QDs film and the H_2O_2 solution-treated film. Both films exhibit a strong visible emission at about 560 nm related to oxygen vacancy defects.[44–46] Almost no obvious near-band-edge (NBE) emission of ZnO can be found in the UV range. Notably, the intensity of the defect emission can be significantly reduced by the H_2O_2 solution treatment, indicating the decrease of oxygen vacancy defects in ZnO QDs. In addition, PLE spectra measured at 550 nm are shown in Fig. 3(b). Clear absorption edges at around 350 nm can be observed for both pristine and the H_2O_2 solution-treated ZnO QDs films.

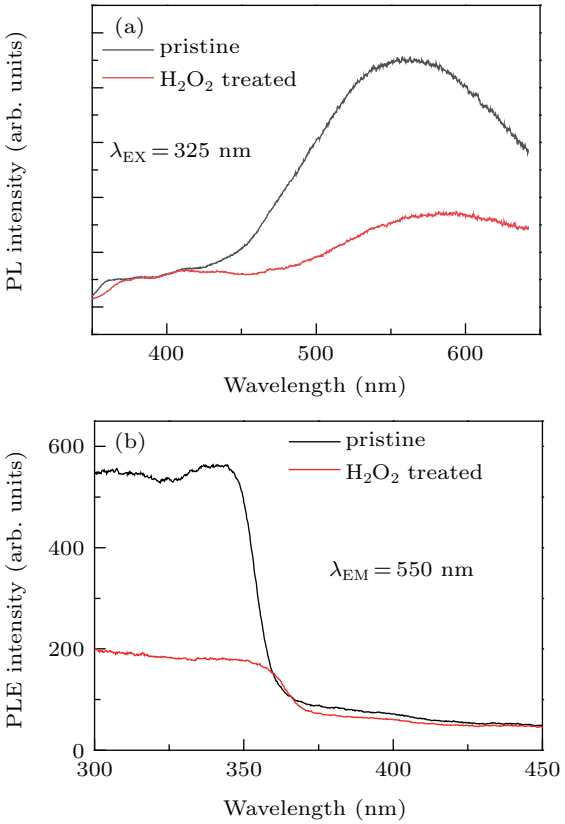


Fig. 3. Room temperature PL (a) and PLE (b) spectra of pristine and H_2O_2 solution-treated ZnO QDs films.

Figures 4(a) and 4(b) display the current–voltage (I–V) curves of the pristine and H_2O_2-treated ZnO QDs detectors in dark and under 365-nm UV illumination. It is obvious that after the treatment by H_2O_2 solution, the dark current of the device decreased and the photocurrent increased. Owing to the large specific surface area of ZnO QDs, surface effects are the main factor affecting the performance of its devices. The H_2O_2 treatment can effectively fill the oxygen vacancy defects on the surface of ZnO QDs, which reducing the concentration of donors. Therefore, the dark current of the H_2O_2-treated device was significantly reduced. As for the increase of the current under the UV light illumination after the H_2O_2 solution treatment, the reduction of photogenerated carrier recombination may be the main reason. As shown in Fig. 4(c), the spectral response of the devices was measured under 10-V bias. It can be seen that the -3-dB cut-off wavelength of two devices is around 340 nm, which is in good agreement

with the PLE spectra as shown in Fig. 3(b). And after the treatment with H_2O_2 solution, the peak resonsivity at around 330 nm increased from 0.03 A/W to 0.24 A/W. The detectivity measuerd in units of Jones (D^*) is given by the following expression:[47,48]

$$D^* = \frac{R}{(2eI_d/S)^{1/2}}, \tag{1}$$

where e is the value of electron charge (1.6×10^{-19} C), I_d is the dark current, and S is the effective illuminated area of the device. After the treatment with H_2O_2 solution, the calculated detectivity at 330 nm increased from 3.8×10^{11} Jones to 6.7×10^{12} Jones.

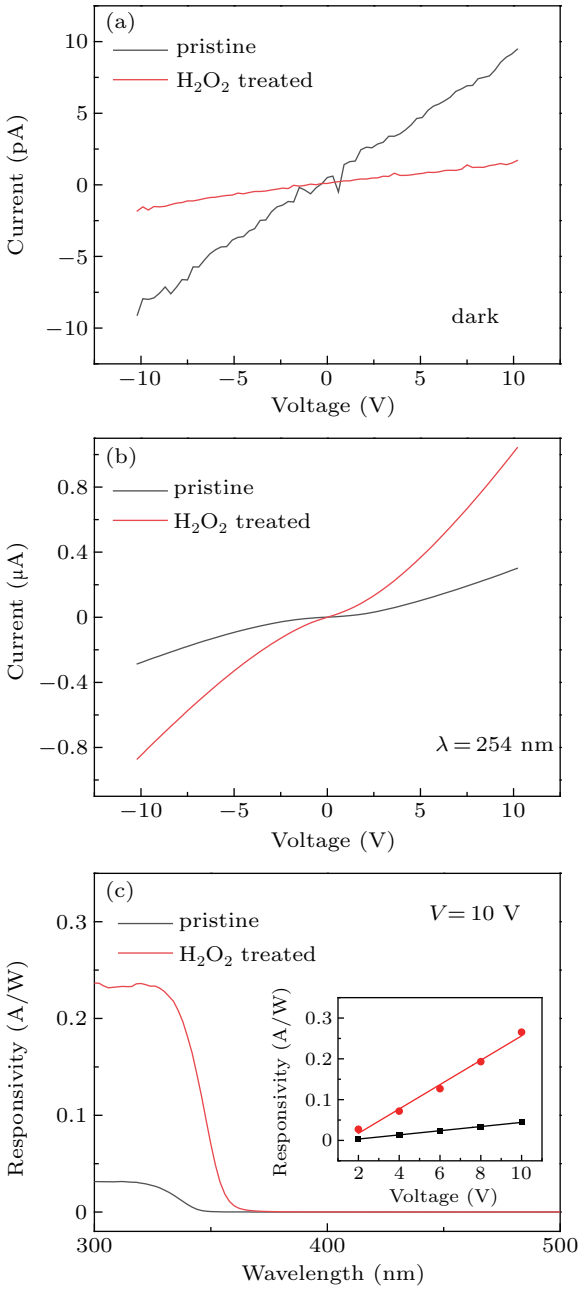


Fig. 4. (a) The dark I–V and (b) photo-I–V curves of the pristine and H_2O_2-treated ZnO QDs detectors. (c) The spectral response of the ZnO QDs detectors under 10 V. The inset shows the variation of peak responsivity at ~ 330 nm *versus* the applied bias.

Besides, as shown in the inset of Fig. 4(c), the peak responsivity of both devices increased almost linearly with the increase of bias voltage from 2 V to 10 V.

In order to investigate the effect of surface V_O defects and the oxygen adsorption/desorption process on the response speed of the ZnO QDs detectors, the time-dependent photocurrent response measurement has been carried out in different atmospheres. Figures 5(a) and 5(b) show the current *versus* time plots of the pristine and H_2O_2-treated ZnO QDs photodetectors under 254-nm UV illumination at 10-V bias in dry air and oxygen atmosphere, respectively. Both devices showed excellent stability and repeatability. As the UV light was turned on, the current of both devices increase to a steady state rapidly. After the UV light was turned off, the current of both devices rapidly dropped and back to its initial level. When the device is working in dry air, the response speed of pristine ZnO QDs detector was obviously quicker than that of the H_2O_2 solution-treated device. Interestingly, when the working atmosphere is changed to pure oxygen, the speed of the two devices has been improved, especially for the H_2O_2 solution-treated device. Figures 5(c) and 5(d) show the decay edges in normalized time-dependent photocurrent of both photodetectors with different temperatures. As shown in Fig. 5(c), the temperature could hardly affect the response speed of the pristine device and the 90%–10% decay times (τ_d) is around 0.08 s at all temperatures. In contrast, as the temperature increased from 17 °C (room temperature) to 110 °C, the 90%–10% decay time of the device treated with the H_2O_2 solution was gradually shortened from 0.7 s to 0.07 s (see Fig. 5(d)). These phenomena can be explained as follows. As is well known, oxygen molecules can be adsorbed on the surface of ZnO and capture the free electrons. Under the UV illumination, electron–hole pairs are generated and the holes would like to be trapped at the surface due to the band bending, which could discharge the adsorbed oxygen ions (O_2 desorption process). After switching off the UV light, oxygen molecules in surrounding atmosphere will be re-adsorbed on the surface ZnO QDs and capture the electrons, which can help the device to restore to the initial dark state. According to the previous reports, oxygen molecules are more likely to chemically adsorb on the surface V_O defects rather than other physical adsorption on the surface.[38,39] Therefore, the pristine ZnO QDs photodetector with more surface oxygen vacancy defects has a faster response speed. Moreover, the adsorption and desorption of oxygen is a dynamic equilibrium process, which depends on the number of oxygen molecules in the surrounding environment and the temperature. Since surface oxygen vacancy defects are easier to chemically adsorb oxygen molecules, the more oxygen vacancies, the lower the dependence on temperature and the concentration of oxygen molecules.

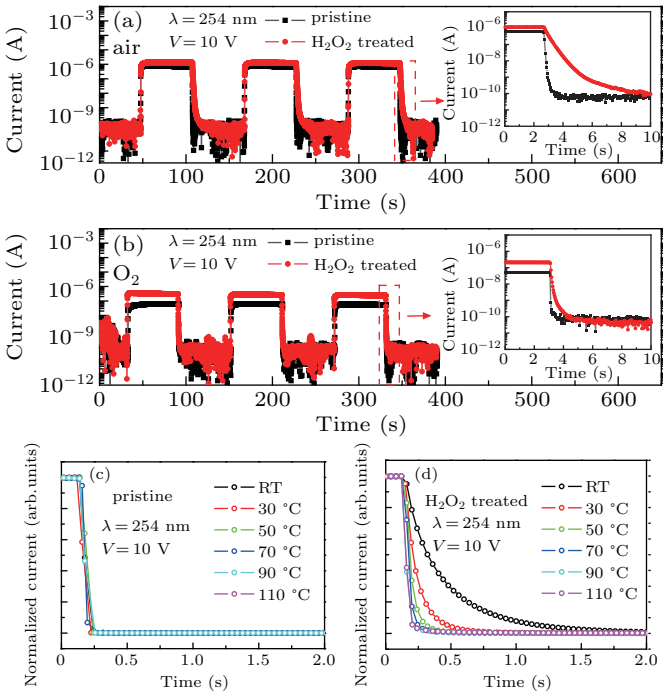


Fig. 5. Time-dependent photocurrent of the pristine and H_2O_2-treated detector by periodic switching of UV illumination (254 nm) under 10 V bias in dry air (a) and (b) O_2. Decay edges of normalized time-dependent photocurrent of the pristine (c) and H_2O_2-treated (d) detectors at different temperatures.

4. Conclusion

In summary, a ZnO QDs film photodetector was fabricated, and then the device was immersed into H_2O_2 solution at room temperature for 5 s. After the H_2O_2 treatment, the defect emission of the material associated with oxygen vacancy was suppressed, which proves that the V_O defects were effectively filled. Meanwhile, the dark current of the device was reduced, while the photocurrent was increased. More interestingly, with the reduction of V_O defects induced by the treatment of H_2O_2 solution, the response speed of the device became slower, and more sensitive to temperature and oxygen concentration. This phenomenon can be attributed to the fact that oxygen molecules are more likely to chemically adsorb on the surface oxygen vacancy defects. This work will provide theoretical guidance for the development of simple, low-cost, and high-speed ZnO QDs UV photodetectors.

References

[1] Lin H W, Ku S Y, Su H C, Huang C W, Lin Y T, Wong K T and Wu C C 2005 *Adv. Mater.* **17** 2489

[2] Mishra Y K, Modi G, Cretu V, Postica V and Lupan O, Reimer T, Paulowicz I, Hrkac V, Benecke W, Kienle L and Adelung R 2015 *ACS Appl. Mater. Interfaces* **7** 14303

[3] Gedamu D, Paulowicz I, Kaps S, Lupan O, Wille S, Haidarschin G, Mishra Y K and Adelung R 2014 *Adv. Mater.* **26** 1541

[4] Zhou H, Fang G J, Liu N and Zhao X Z 2011 *Mater. Sci. Eng. B* **176** 740

[5] Shaikh S K, Inamdar S I, Ganbavle V V and Rajpure K Y 2016 *J. Alloys Compd.* **664** 242

[6] Xuan J Y, Zhao G D, Shi X B, Geng W, Li H Z, Sun M L, Jia F C, Tan S G, Yin G C and Liu B 2021 *Chin. Phys. B* **30** 020701

[7] Yang J L, Liu K W and Shen D Z 2017 *Chin. Phys. B* **26** 047308

[8] Zhou C, Ai Q, Chen X, Gao X, Liu K and Shen D 2019 *Chin. Phys. B* **28** 048503

[9] Yu X X, Zheng H M, Fang X Y, Jin H B and Cao M S 2014 *Chin. Phys. Lett.* **31** 117301

[10] Liu K, Sakurai M and Aono M 2010 *Sensors* **10** 8604

[11] Pearton S, Norton D, Ip K, Heo Y and Steiner T 2004 *J. Vac. Sci. Technol. B* **22** 932

[12] Look D C 2001 *Mater. Sci. Eng. B* **80** 383

[13] Ohtomo A, Kawasaki M, Sakurai Y, Yoshida Y, Koinuma H, Yu P, Tang Z K, Wong G K L and Segawa Y 1998 *Mater. Sci. Eng. B* **54** 24

[14] Hatch S M, Briscoe J and Dunn S 2013 *Adv. Mater.* **25** 867

[15] Li L, Gu L, Lou Z, Fan Z and Shen G 2017 *ACS Nano* **11** 4067

[16] Litvin A P, Martynenko I V, Purcell-Milton F, Baranov A V, Fedorov A V and Gun'ko Y K 2017 *J. Mater. Chem. A* **5** 13252

[17] Tian W, Lu H and Li L 2015 *Nano Res.* **8** 382

[18] Li X, Li X, Zhu B, Wang J, Lan H and Chen X 2017 *RSC Adv.* **7** 30956

[19] Hoang Tran M, Park T and Hur J 2021 *Appl. Surf. Sci.* **539** 148222

[20] Chen Z, Li X X, Du G, Chen N and Suen A Y M 2011 *J. Lumin.* **131** 2072

[21] Debasis, Bera, Lei, Qian, Subir, Sabui and Swadeshmukul 2008 *Opt. Mater.* **30** 1233

[22] Liu Y, Morishima T, Yatsui T, Kawazoe T and Ohtsu M 2011 *Nanotechnology* **22** 215605

[23] Jin Y Z, Wang J P, Sun B Q, Blakesley J C and Greenham N C 2008 *Nano Lett.* **8** 1649

[24] Yan W, Mechau N, Hahn H and Krupke R 2010 *Nanotechnology* **21** 115501

[25] Mishra S K, Srivastava R K and Prakash S G 2012 *J. Mater. Sci.: Mater. Electron.* **24** 125

[26] Nasiri N, Bo R, Wang F, Fu L and Tricoli A 2015 *Adv. Mater.* **27** 4336

[27] Guo D Y, Shan C X, Qu S N and Shen D Z 2014 *Sci. Rep.* **4** 7469

[28] Liu S, Li M Y, Su D, Yu M, Kan H, Liu H, Wang X and Jiang S 2018 *ACS Appl. Mater. Interfaces* **10** 32516

[29] Abbasi F, Zahedi F and Yousefi M H 2021 *Opt. Commun.* **482** 126565

[30] Liu S, Li M-Y, Zhang J, Su D, Huang Z, Kunwar S and Lee J 2020 *Nano-Micro Lett.* **12** 114

[31] Li M Y, Yu M, Su D, Zhang J, Jiang S, Wu J, Wang Q and Liu S 2019 *Small* **15** 1901606

[32] Xu X, Xu C and Hu J 2014 *J. Appl. Phys.* **116** 103105

[33] Tian W, Zhang C, Zhai T, Li S L, Wang X, Liao M, Tsukagoshi K, Golberg D and Bando Y 2013 *Chem. Commun. (Camb)* **49** 3739

[34] Jeon S, Ahn S E, Song I, Kim C J, Chung U I, Lee E, Yoo I, Nathan A, Lee S, Robertson J and Kim K 2012 *Nat. Mater.* **11** 301

[35] Ahn S E, Ji H J, Kim K, Kim G T, Bae C H, Park S M, Kim Y K and Ha J S 2007 *Appl. Phys. Lett.* **90** 153106

[36] Guo W, Xu S, Wu Z, Wang N, Loy M M and Du S 2013 *Small* **9** 3031

[37] Bera A and Basak D 2009 *Appl. Phys. Lett.* **94** 163119

[38] Li G, Zhang H, Meng L, Sun Z, Chen Z, Huang X and Qin Y 2020 *Sci. Bull.* **65** 1650

[39] An W, Wu X and Zeng X C 2015 *J. Phys. Chem. C* **112** 5747

[40] Zhang B, Li M, Wang J Z and Shi L Q 2013 *Chin. Phys. Lett.* **30** 027303

[41] Zhu Y, Liu K, Wang X, Yang J, Chen X, Xie X, Li B and Shen D 2017 *J. Mater. Chem. C* **5** 7598

[42] Kwoka M, Kulis-Kapuscinska A, Zappa D, Comini E and Szuber J 2020 *Nanotechnology* **31** 465705

[43] Chen M, Wang X, Yu Y H, Pei Z L, Bai X D, Sun C, Huang R F and Wen L S 2000 *Appl. Surf. Sci.* **158** 134

[44] Choi S, Phillips M R, Aharonovich I, Pornsuwan S, Cowie B C C and Ton-That C 2015 *Adv. Opt. Mater.* **3** 821

[45] Zeng H, Duan G, Li Y, Yang S, Xu X and Cai W 2010 *Adv. Funct. Mater.* **20** 561

[46] Tang X S, Choo E S G, Li L, Ding J and Xue J M 2010 *Chem. Mater.* **22** 3383

[47] Wang Y, Wang P, Zhu Y, Gao J, Gong F, Li Q, Xie R, Wu F, Wang D, Yang J, Fan Z, Wang X and Hu W 2019 *Appl. Phys. Lett.* **114** 011103

[48] Jiang W, Zheng T, Wu B, Jiao H, Wang X, Chen Y, Zhang X, Peng M, Wang H, Lin T, Shen H, Ge J, Hu W, Xu X, Meng X, Chu J and Wang J 2020 *Light Sci. Appl.* **9** 160